

Chaotic Bloch oscillations in driven-dissipative systems

A. Verbitsky and A. Yulin

*School of Physics and Engineering, ITMO University,
Kronverksky Pr. 49, bldg. A, St. Petersburg, 197101, Russia*

(Dated: June 30, 2022)

It is shown that the efficiency of the excitation of Bloch oscillations depends not only on the carrier frequency, but also on the frequency of the amplitude oscillations of the driving force. In the nonlinear regime a period doubling bifurcation occurs and the chain of these bifurcations results in chaotic Bloch oscillations of the wave envelope bouncing in the system.

I. INTRODUCTION

Bloch oscillations is a very interesting physical phenomenon first discovered during the development of zone theory of the solid state physics [1–3]. The effect consist in the periodic motion of an electron (or another quantum particle) moving in a combination of a periodic (lattice potential) and a linear (constant electric field) potentials. The theoretical discovery was followed by a long scientific discussion and finally the effect was confirmed experimentally [4–7], see also review [8].

It is well known that, under some conditions, the dynamics of light is described by the same equations as the wave function of particles in quantum mechanics. Therefore it is reasonable to anticipate that an optical analogue of Bloch oscillations can be found in optical systems. Indeed, optical Bloch oscillations have been predicted in optical waveguide arrays and photonic crystals [9–13]. In that systems the effective refractive index depends linearly on a spatial coordinate and this plays a role of a linearly growing part of the potential in quantum systems. The spectrum of the eigenmodes of these systems is equidistant (have a form of Wannier-Stark ladder) and the light propagates along snake-like trajectories.

Optical Bloch oscillations are much easier to observe experimentally compared to their quantum counterparts and thus their theoretical discovery was accompanied by a number of experimental works where Bloch oscillations were demonstrated [9, 14–20]. A comprehensive review on optical Bloch oscillations, Zener tunneling and related effects can be found in [21]. It is important to acknowledge that Bloch oscillations are a very generic effect and occur in a large number of physical systems such as atomic systems [22–27], lasers [28], coupled LC circuits [29], mechanical systems [30–33], plasmonic [34–39] or exciton-polariton systems [40–42].

Bloch oscillations is a linear phenomenon but, of course, nonlinearities of the physical systems can affect Bloch oscillations. In most cases the effect of the nonlinearity on the Bloch oscillations is destructive making it impossible to observe the oscillations at long times [43–48]. The main reason why nonlinear effects prevent observation of long-living Bloch oscillations is modulation instability appearing when the envelope approaches the edges of the band [49]. This understanding allowed to suggest different, sometimes quite complicated methods

of nonlinearity management stabilizing Bloch oscillations in the nonlinear regime [50–53]. It was also found that, quite surprisingly, the increase of the dimensionality of the system can also stabilize Bloch oscillations [54] making possible, for instance, their use for resonant new frequency generation [55].

The aim of the present paper is to study nonlinear regimes of optical Bloch oscillations in a system of interacting cavities pumped by a periodic train of external coherent pulses. It will be shown that the excitation efficiency greatly increases when the period of pump pulses train coincides with a frequency of Bloch oscillations. In the presence of coherent pump the dephasing of the Wannier-Stark states due to nonlinear effects can be safely neglected if the dephasing time is much longer compared to the lifetime of the waves excited in the system. Much of the attention is paid to period doubling bifurcation that occurs in the system when the intensity of the excited field exceeds some threshold.

We will show that a sequence of period doubling bifurcation can destroy the periodicity of Bloch oscillations completely. Deterministic chaos has been studied for decades and is widely discussed in vast literature on nonlinear dynamics, see, for example, review [56] devoted to chaotic behaviour of different oscillators. It is also known that deterministic chaos can appear in the systems described by nonlinear Schrodinger equation [57–60]. The focus point of our work is the specific effect of the chaotization of the Bloch oscillation appearing due to Kerr nonlinearity in the system. We believe that the reported result may contribute to better understanding of the physics of Bloch oscillations and may find practical application, for example, in new frequencies generation in optical systems.

We consider a simple system consisting of a one-dimensional array of coupled single-mode resonators. The schematic view of the resonator array is given in Fig. 1. The resonators can be pumped by pulses of external coherent light of finite spatial aperture launched at some angle to the resonator array. The resonators are coupled to free propagating waves which means that the resonator modes are leaky and the resonators experience radiative losses. The total losses are the sum of the radiative and Joule losses and are characterized by an effective dissipation rate. To achieve Bloch oscillations in the system we make the resonant frequency of

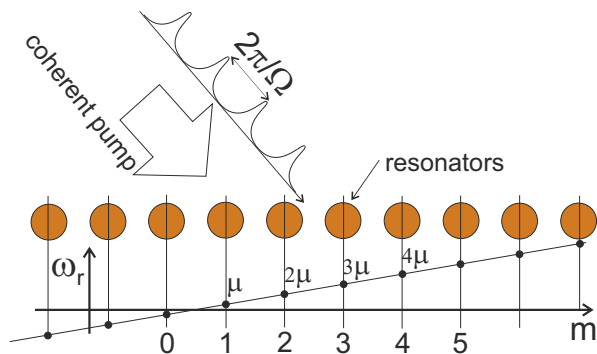


FIG. 1. (Color online) The schematic view of the array of optical resonators pumped by a train of coherent pulses. The resonant frequencies of the resonators depend on their indexes linearly.

the resonators to be a linear function of the index numbering the resonators. First, we consider the case where the resonant frequency of the resonators depends on the intensity of the field in the resonators and in the leading approximation the shift of the resonant frequency is proportional to the intensity of the mode. We consider the case of instantaneous nonlinearity. The simplest realization of such systems is an array of conventional optical nonlinear resonators.

To study the influence of the nonlinear losses on the dynamics of the system we consider a polaritonic system consisting of interacting micro-pillars pumped simultaneously by incoherent and coherent pumps. The incoherent pump is needed to control the effective losses seen by the polaritons. To study the nonlinear effects it is convenient to have high-Q resonators and this can be achieved

$$i\partial_t u_n = \left(\mu n - \hat{D} - i\gamma + \alpha |u_n|^2 \right) u_n + a_n \exp(i\omega_p t - ik_p n), \quad (1)$$

where n enumerates the resonators, the operator $\hat{D}u_n = \sigma(u_{n+1} + u_{n-1} - 2u_n)$ accounts for the coupling between the neighbouring resonators, γ is linear losses, μ characterizes the steepness of the linear dependency of the eigenfrequency of the resonators on their number, a_n is the amplitude of the pump, ω_p is the detuning of the pump frequency from the resonance frequency of the resonator with $n = 0$, k_p is the projection of the phase gradient of the pump field on the axis passing through the resonators array, $a_n(t)$ is the complex amplitude of the pump coming to n -th resonator. For the sake of mathematical convenience we introduce dimensionless units.

We use the aperture of the excitation beam that is much smaller than the span of Bloch oscillations. At the same time, we require that the aperture be wide enough

by applying a proper incoherent pump. However, in this paper we keep the pump below the threshold. Another reason to consider a polariton system is that such systems exhibit very strong Kerr nonlinearity facilitating experimental investigation of the nonlinear effects.

The paper is structured as follows. In the next section we consider a mathematical model capable to describe Bloch oscillations in driven-dissipative systems. In this section we discuss a linear regime of Bloch oscillations and show that the efficient excitation takes place when the field intensity is varying with the frequency equal to the frequency of Bloch oscillations. In the third section the nonlinear propagation of the field is considered. It is shown that the nonlinearity brakes the symmetry of the field propagating in the system. Chaotic behaviour of the system is also discussed in this section. The fourth section is devoted to nonlinear dynamics of polariton systems. It is shown that period doubling bifurcation takes place in polariton systems too. The main results of the paper are briefly summarized in the conclusion.

II. LINEAR REGIME OF BLOCH OSCILLATIONS IN AN ARRAY OF COHERENTLY DRIVEN RESONATORS

We start with a simple model describing an array of coupled optical resonators, see Fig. 1. We assume that the inter-resonator coupling, losses and the nonlinear effects do not change the structure of the field in each of the resonator, but affect the amplitudes and the phases of the resonator modes. So a tight-binding approximation can be used and the field in each of the resonator can be characterized by a slowly varying complex amplitude u . Then the dynamics of the system is described by a discrete dissipative nonlinear Schrodinger equation (DDNLS) written for the complex amplitudes of the resonator modes

so that its spatial spectrum is narrow compared to the Brillouin zone. In our numerical simulation we took the aperture to be equal to $w = 5$. Then considering the dynamics in the excitation spot we can neglect the dependency of the resonant frequency on the index of the resonator. In this case a single pulse excites a propagating envelope efficiently if the frequency and the wavevector of the pump are related as $\omega_p = 2\sigma(1 - \cos(k_p)) + \mu n_p$, where n_p is the position of the pump centre. Without loss of generality we pump at $n_p = 0$. In the examples of numerical simulations presented in the paper the pump frequency is chosen to be in the middle of the zone, so $\omega_p = 2\sigma$, $k_p = \pi/2$. The variation of the amplitude of the pump exciting the system we take in the form $a_n(t) = a_p |\sin(\Omega t)|^7 \exp(-n^2/w^2)$, where Ω is the fre-

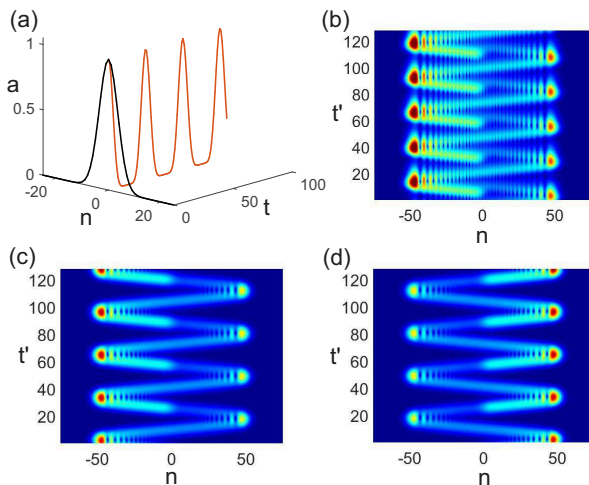


FIG. 2. (Color online) (a) the dependencies of the normalized driving force amplitude $a(n, t = 0)$ and $a(n = 0, t)$. The evolution of the field $u_n(t)$ in stationary regime are shown in panels (b) and (c) for the frequency of driving force amplitude $\Omega = 0.2$ and $\Omega = 0.1$ correspondingly. (d) is the same as (c) but for the opposite sign of the driving force wave vector, $k_p = -\pi/2$. The amplitude of the driving force is small to insure linear regime of propagation. The other parameters are $\gamma = 0.025$, $\mu = 0.2$

quency of the pump intensity variation. The spatial distribution and the temporal evolution of the normalized driving force amplitude is shown in Fig. 2.

The linear regimes of propagation are illustrated in Fig. 2. Each pulse of the pump excites a wave envelope experiencing Bloch oscillations. If the frequency of the pump pulses does not coincide with the frequency of Bloch oscillations then the waves excited by different pulses do not interfere constructively (panel (b) of Fig. 2). The constructive interference occurs at $2\Omega = m\mu$, where m is an integer, see panel (c). This can be seen as a resonance between the pump and the Bloch oscillations.

It should also be noted that in the linear regime there is no difference between the excitation of the pulses propagating from the right to the left and the pulses propagating from the left to the right, compare the panels (c) and (d) corresponding to pump wavevectors of the opposite signs. Another important remark to be made is that the oscillations are well localized in the linear regime.

To lit more light on the Bloch resonance we calculated the maximum amplitude of the stationary field as a function of the frequency of the driving force amplitude. The results are presented in Fig. 3 showing the resonance curve for different losses. The maxima corresponding to the resonances are well developed even for relatively large losses.

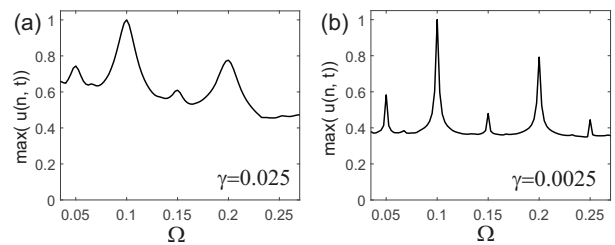


FIG. 3. (Color online) The resonance curves showing the dependency of the maximum amplitude of the stationary field on the frequency of the driving force amplitude Ω for relative large losses $\gamma = 0.025$ (a) and for smaller losses $\gamma = 0.0025$. The amplitude of the driving force is very low so the the problem is linear.

III. NONLINEAR EVOLUTION OF THE FIELD OF DRIVEN BLOCH OSCILLATIONS

Now let us consider how the dependency of the resonant frequencies of the resonators on the field intensity affect the dynamics of the system. The first important observation is that in the nonlinear regime the symmetry $k_p \rightarrow -k_p$ is broken. In Fig. 4 the stationary stages of field propagation are shown for $k_p = \pm\pi/2$ in the case of very intense pumping $a_p = 0.8$. It is clearly seen that the dynamics is very different. For lower pump intensity the asymmetry also takes place but is not that pronounced.

It is also worth mentioning that in the strong nonlinear regime the localization of the field become larger. The spreading of the field cannot be explained by the inter-band tunneling because the dispersion has only one branch. The generation of the new waves gives rise to the formation of numerous snakes of Bloch oscillations.

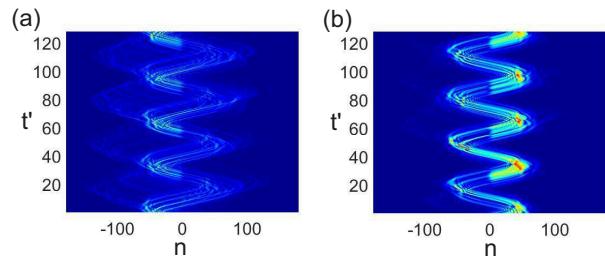


FIG. 4. (Color online) The stationary evolutions of the field in strongly nonlinear regime $a_p = 0.8$ for $k_p = \pi/2$ (a) and $k_p = -\pi/2$ (b).

Let us now study in more detail what happens to the dynamics of the field when the driving force amplitude increases. The evolution of the field excited by the driving force of the amplitude $a_p = 0.3$ is shown in panel (a) of Fig. 5. It is seen that the period of the temporal oscillations became twice of that in the linear regime. To make it even more obvious we plotted the dependency of the amplitude of the field at site $n = -48$ as a function of time for the pump $a_p = 0.3$, see panel (b) of Fig. 5.

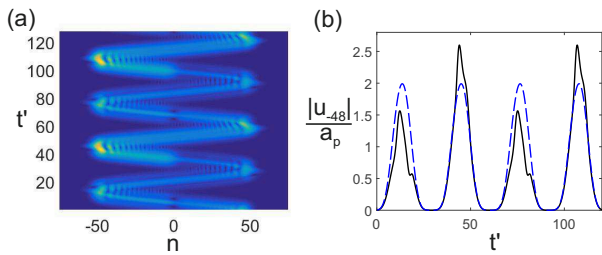


FIG. 5. (Color online) (a) The stationary evolution of the field for the pump amplitude $a_p = 0.3$. The temporal evolution of the absolute value of the field at the site $n = -48$ is shown in panel (b) by solid black line. The dashed blue line shows the evolution of the field amplitude at the same site for the pump amplitude $a_p = 0.2$. For convenience both amplitudes are normalized on the amplitude of the pulse a_p .

For reference we plotted the same dependence but for the pump $a_p = 0.2$ by the blue line. The pump $a_p = 0.2$ is already nonlinear regime, but the period is the same as in the linear regime. This gives a reason to suggest that the period doubling bifurcation takes place in the system. Below we prove that this indeed what happens in the system and that a chain of period doublings results in the chaotic behaviour of the system.

Our system can be seen as a dynamical system whose phase space has a dimension equal to $2N$, where N is the number of sites in the system. To study the period doubling bifurcation it is instructive to calculate the phase trajectories and to plot the projection of the phase trajectory (PPT) on two-dimensional phase space. The periodic motion corresponds to a closed loop of the PPT. Then the period doubling manifests itself by the splitting of the loop into two closed loops.

We choose the plotted quantities to be the energy $W = \sum_n |u_n|^2$ and momentum $M = \text{Im}(\sum u_n^* \cdot (u_{n-2} - u_{n-1}))$. It is convenient to plot the trajectories in the axes W/a_p^2 and M/a_p^2 because in the linear regime both W and M are proportional to a_p^2 . This means that the trajectory plotted in the chosen coordinates does not depend on the pump and has a shape as the one calculated for $a_p = 0.001$, see Fig. 6.

In slightly nonlinear regime the shape of the trajectory does not change qualitatively but its span decreases, see the trajectory calculated for $a_p = 0.24$. This is so until the pump amplitude exceeds a threshold value. Then the trajectory makes a twist, and now it can be considered as consisting of two similar loops, see the trajectory calculated for $a_p = 0.246$. This is a characteristic feature of period doubling bifurcation. At higher pumps the trajectory continues to deform, see the one calculated for $a_p = 0.3$. Then another period doubling bifurcation occurs, see the trajectory calculated for $a_p = 0.31$. Finally, these period doubling bifurcations result in very complex behaviour, see the trajectory calculated for $a_p = 0.35$.

Let us discuss the temporal spectra of the field. We took a stationary variation of the field at site $n = -48$

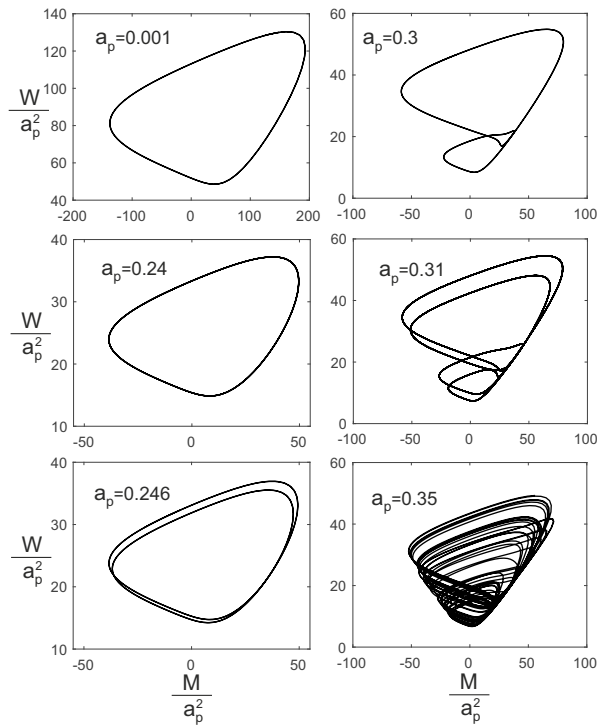


FIG. 6. (Color online) The projections of the phase trajectories onto the phase plane ($W = \sum_n |u_n|^2$; $M = \text{Im}(\sum u_n^* \cdot (u_{n-2} - u_{n-1}))$) for different amplitudes of the resonant pump a_p . The other parameters are the same as in Fig. 5

and calculated its spectra for different levels of the pump, see Fig. 7. Initially the spectrum contains the carrier frequency and the harmonics detuned from the carrier frequency by the frequency of the oscillations of the pump amplitude. After the period doubling subharmonics appear. These subharmonics at the frequencies $l\Omega/2$, where l is an integer, indicate that the period of the oscillations becomes twice of the period of the driving force. Then the next period doubling bifurcation produces the subharmonics at the frequencies $l\Omega/4$. Finally, we arrive to the spectrum of the chaotic signal consisting of two parts: the continuous background overlapped with the discrete spectrum. The first one corresponds to the chaotic part of the field and the second one - to the regular component of the field that can be seen as direct response of the system to the driving force. Let us note that, of course, the number of harmonics defines the shape of the field, but not its period.

It is also instructive to calculate the correlation function of the field defined as

$$\Gamma(\tau, \xi) = \lim_{T \rightarrow \infty} \lim_{N \rightarrow \infty} \frac{1}{4NT} \sum_{n=-N}^N \int_{-T}^T u_{n-\xi}(t-\tau) \cdot u_n(t) dt.$$

The correlation function is calculated by the averaging over a large window where the signal is stationary. In numerics the function depends on the position of the av-

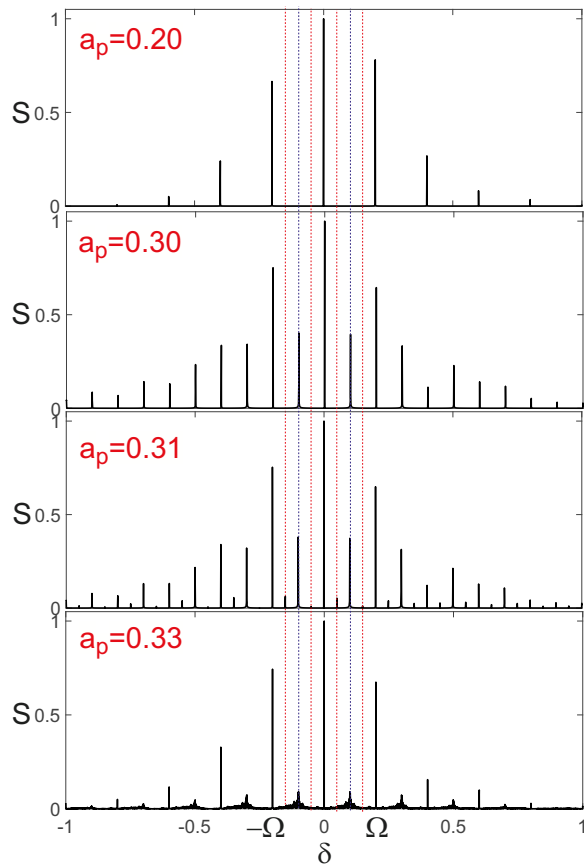


FIG. 7. (Color online) Temporal spectra of the field at site $n = -48$ for different amplitudes of the driving force a_p . Dashed blue and red lines show the positions of several first subharmonics at $l\Omega/2$ and $l\Omega/4$. The horizontal axis is $\delta = \omega - \omega_p$ the detuning of the frequency from the carrier frequency of the pump.

eraging window, but we have checked that this difference is small. The correlation functions are shown in Fig. 8 for $a_p = 0.4$.

It is seen that the correlation function is well localized along the discrete coordinate, this is so because the field is well localized along the discrete coordinate. It is more interesting how the correlation functions changes with time. The dependencies of the correlations on time are shown in panels (b) for different regimes of the field propagation. It is seen that that for low pumps the correlation function is periodic. After the period doubling the period of the correlation function also becomes doubled. In the chaotic regime the correlation function rapidly drops down to some (actually, quite high) background existing because the total field contains not only chaotic, but also a periodic component.

It is also possible to calculate Poincare section and to plot Feigenbaum diagrams to trace the period doubling bifurcations and the transition to chaos. We traced the points where the phase trajectories cross the hypersurface $t = 2m\pi/\Omega$ and plotted the energy W of the field

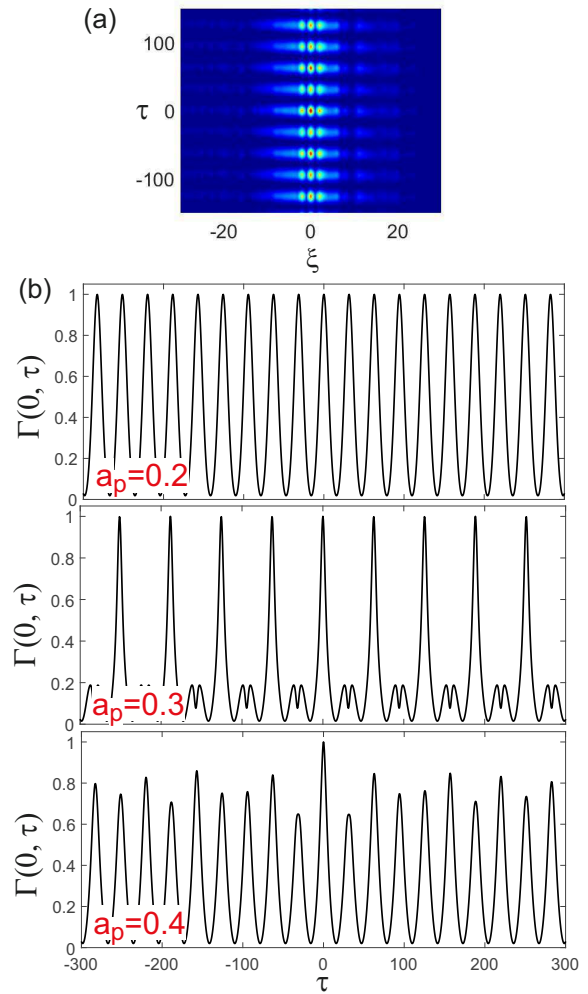


FIG. 8. (Color online) (a) Two-dimensional correlation function calculated for the stationary field for driving force amplitude $a_p = 0.4$. The sections of the two-dimensional correlation functions $\Gamma(\xi = 0, \tau)$ for different pump amplitudes are shown in panel (b).

at these points. Doing this for different values of the pump amplitudes a_p we obtain the Feigenbaum diagram shown in Fig. 9. One can clearly see three first period doubling bifurcation points and then the transition to chaotic regime.

So now we can conclude that in the presence of conservative cubic nonlinearity the resonantly excited Bloch oscillations of the coherent light can switch to chaotic regime via period doubling bifurcation. Now let us study how dissipation (including the nonlinear one) affects this phenomenon. For this purpose we consider a polariton system that possesses high nonlinearity due to strong light matter coupling and can be seen as a promising system where the discussed effects may be observed.

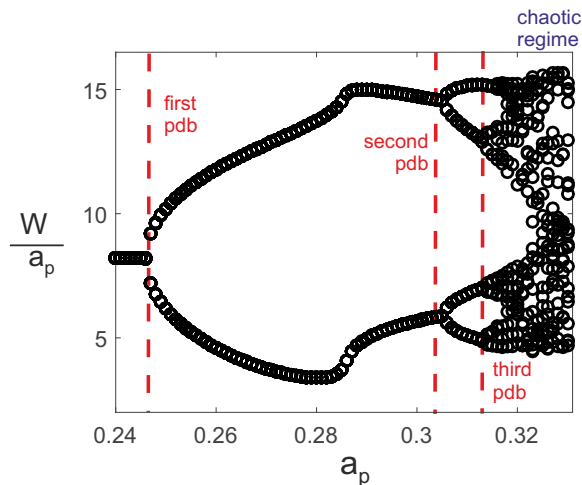


FIG. 9. (Color online) The figure shows the Feigenbaum diagram calculated for the resonantly pumped Bloch oscillations in the system of coupled oscillators described by (1). The vertical axis is the energy $W = \sum_n |u_n|^2$ normalized on the pump amplitude a_p for the point where the phase trajectory crosses the hyper-surface defined by the condition $t = 2m\pi/\Omega$, the horizontal axis is the pump. The positions of the first three period doubling bifurcations (pdb) are marked by the dashed red vertical lines and labeled with "first pdb", "second pdb" and "third pdb" correspondingly.

IV. POLARITONS

We can think about similar phenomenon in other driven-dissipative systems exhibiting Bloch oscillations in the linear regime. One of the important example of such systems is a coupled semiconductor microcavities supporting exciton-polaritons. The systems of this kind are promising for experimental verification of the effect because they are highly nonlinear and allow to control effective linear losses making them small enough. To describe the polariton dynamics we use the widely accepted model consisting of the equation for the order parameter of the polariton field ψ and the density of incoherent excitons ρ

$$i\partial_t\psi_n = \left(\mu n - \hat{D} - i\gamma_1 + i\rho_n + |\psi_n|^2 + \alpha\rho_n\right)\psi_n + Q_n \exp(i\omega_p t - ik_p n), \quad (2)$$

$$\partial_t\rho_n = -(\gamma_2 + \beta|\psi_n|^2)\rho_n + P_n. \quad (3)$$

where $\hat{D}\psi = \sigma(\psi_{n+1} + \psi_{n-1} - 2\psi_n)$ is the operator of the discrete diffraction, γ_1 is the losses for the coherent polaritons, α accounts for the blue shift of the coherent polaritons due to their nonlinear interaction with the incoherent ones, γ_2 is the losses in the incoherent polaritons subsystem, β define the additional damping rate of the incoherent polaritons caused by their condensation into the coherent polaritons, P_n is the amplitude of the incoherent pump, μ is the gradient of the resonant frequency, $Q_n(t)$ is the amplitude of the coherent pump, ω_p its frequency and k_p is its wave vector. We use dimensionless units normalizing the time by the typical for such systems characteristic time 10 ps; the polariton density is normalized by the characteristic polariton density $\frac{\hbar}{g_c\tau}$ where g_c is characteristic polariton-polariton interaction constant; the density of the incoherent exciton reservoir is normalized on $\frac{2}{R\tau}$ where R is the condensation rate; $\alpha = \frac{2g_r}{\hbar R}$ where g_r is the coefficient characterizing the blue shift of the polariton frequency proportional to the incoherent excitons density; $\gamma_2 = \Gamma_x\tau$ where Γ_x is the relaxation rate of the reservoir; $\beta = \frac{\hbar R}{g_c}$. We take typical polariton parameters $g_c = 1.2 \cdot 10^{-3} \text{ meV} \cdot \mu\text{m}^2$, $R = 0.001$

$\text{ps}^{-1} \cdot \mu\text{m}^2$, $g_r = 2.4 \cdot 10^{-3} \text{ meV} \cdot \mu\text{m}^2$, $\Gamma_x = 3 \text{ ps}^{-1}$.

We performed numerical simulations for a realistic polariton decay rate $\tau = 25 \text{ ps}$, so the dimensionless constants are $\gamma_1 = 0.4$, $\alpha = 7.3$, $\gamma_2 = 3.3$, $\beta = 0.55$. The dimensionless coupling strength between polariton pillars is chosen to be $\sigma = 5$ (0.5 ps^{-1} in physical units), the difference in resonant frequencies in the neighbouring pillars is 0.2 (0.02 ps^{-1} in physical units). Let us remark that the polariton losses are too high for convenient observation of Bloch oscillation, but the losses can be compensated by the the reservoir created by the incoherent pump. Therefore we consider the case where the incoherent excitons density is close to the condensation threshold (which is ρ_{th} in dimensionless units).

For our numerical modeling we take the coherent pump in the same form as before $Q_n = a_p |\sin(\Omega t)|^7 \exp(-n^2/w^2)$. We calculated Feigenbaum diagrams for different incoherent pumps controlling the effective losses seen by the polaritons. Two examples are shown in Fig. 10 for the incoherent pump slightly below the lasing threshold so that the effective linear losses seen be the polaritons are low being equal to $\gamma_{eff lin} = 0.0125$ for panel (a) and $\gamma_{eff lin} = 0,025$ for panel (b). The fre-

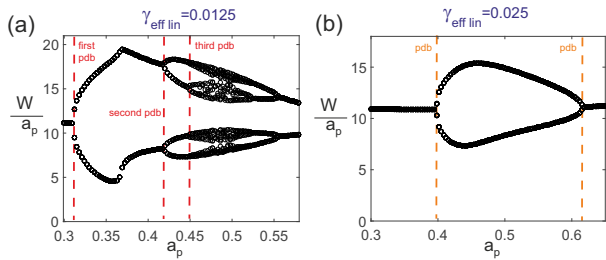


FIG. 10. (Color online) Panel (a) shows a Feigenbaum diagram for the exciton-polariton system simultaneously pumped by the coherent and incoherent light. The incoherent pump is below but close to lasing threshold so that linear polaritons see effective losses $\gamma_{eff lin} = 0.0125$ for panel (a) and $\gamma_{eff lin} = 0.025$ for panel (b). The vertical axis is the energy of the field $W = \sum_n |\psi_n|^2$ divided by the pump amplitude a_p for the point where the phase trajectory crosses the hypersurface defined by the condition $t = 2\pi m/\Omega$, the horizontal axis is the coherent pump amplitude a_p . The positions of the period doubling bifurcations (pdb) are marked by the dashed red (in panel (a)) and orange (in panel (b)) vertical lines.

quency of the coherent pump is chosen to be in resonance with the linear polaritons. Let us note that this resonant frequency depends on the intensity of incoherent pump and thus the frequency of the pump is slightly different for panels (a) and (b). It is seen that for polariton systems the period doubling bifurcation occurs and in this sense the polariton systems are similar to the systems considered above.

The important difference, however, is that in the polariton system the chaotic regime can be achieved only if the pump is extremely close to the lasing threshold, which means very low linear losses. For the higher losses, as it is seen in Fig. 10(b), the increase of the pump results in the stabilization of Bloch oscillations, so that the initial period of the oscillations gets restored and becomes equal to the period of the driving force.

The dynamics of the field amplitude is illustrated in Fig. 11 showing the evolution of the field for the pump amplitudes $a_p = 0.38$, $a_p = 0.5$ and $a_p = 0.675$. It is seen that for $a_p = 0.38$ all Bloch oscillations are identical whereas for $a_p = 0.5$ the odd and the even Bloch oscillations become different. For the even higher pump $a_p = 0.675$ Bloch oscillations are identical again. Comparing panels (b) and (d) one can conclude that the dynamics of the fields excited by pumps $a_p = 0.38$ and $a_p = 0.675$ are very similar.

So we can summarize that resonantly excited Bloch oscillations may be observed in polariton systems for the parameters achievable in the experiment. It is also possible to observe period doubling bifurcations in these settings, however to achieve chaotic dynamics the polariton systems have to be very close to the lasing threshold which can complicate the observation of this effect in real experiments.

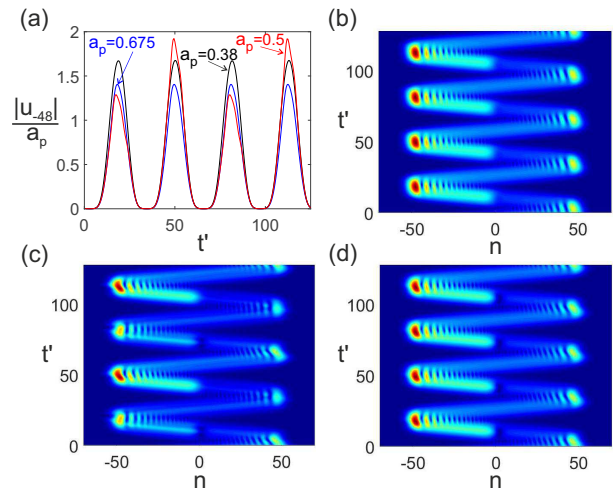


FIG. 11. (Color online) The dependencies of the normalized amplitudes of the field in site $n = -48$ on time are shown in panel (a) for the polaritons driven by the resonant coherent pump with the amplitudes $a_p = 0.38$ (black line), $a_p = 0.5$ (red line) and $a_p = 0.675$ (blue line). Panel (b), (c) and (d) show spatial-temporal evolution of the field for $a_p = 0.38$, $a_p = 0.5$ and $a_p = 0.675$ correspondingly. The incoherent pump is chosen to provide effective losses $\gamma_{eff lin} = 0.025$ in the linear regime of polaritons propagation.

V. CONCLUSION

In this paper we consider Bloch oscillations in the nonlinear driven-dissipative systems with Kerr nonlinearity. It is shown that in the linear regime the evolution of the field does not depend on the sign of the wavevector of the driving force. The efficiency of the excitation of the Bloch oscillations depends not only on the frequency of the field (temporal derivative of the phase of the field at a fixed site), but also on the period of the pulses in the pulse train pumping the system. The maximum efficiency is achieved when the delay between the pulses is equal to the inverse Bloch frequency multiplied by 2π .

The nonlinearity brakes the symmetry in the sense that the pulses launched in one direction propagate differently than the pulses launched in the opposite direction. More importantly, the nonlinearity causes period doubling bifurcation and the sequence of these bifurcations makes the Bloch oscillations to be chaotic. The field evolution can still be seen as Bloch oscillations, but every round of the oscillations is characterized by a different intensity of the field.

It is shown that coherently driven Bloch oscillations can be observed in exciton-polariton systems with experimentally achievable parameters. The period doubling bifurcation can occur in this system. However, to achieve chaotic motion the incoherent pump has to be very close to lasing threshold which can complicate the observation of the chaotic Bloch oscillations in polariton systems.

ACKNOWLEDGEMENTS

This research was supported by Priority 2030 Federal Academic Leadership Program and by the Ministry

of Science and Higher Education of Russian Federation, goszadanie no. 2019-1246.

-
- [1] F. Bloch, Uber die Quantenmechanik der Elektronen in Kristallgittern, *Z. Phys.* 52, 555 (1929).
- [2] C. Zener, A theory of the electrical breakdown of solid dielectrics, *Proc. R. Soc. A* 145, 523 (1934).
- [3] W.V. Houston, Acceleration of electrons in a crystal lattice, *Phys. Rev.* 57, 184 (1940).
- [4] A. Rabinovitch, and J. Zak, Does a Bloch electron in a constant electric field oscillate? *Phys. Lett. A* 40, 189 (1972).
- [5] J. Zak, Comment on Time evolution of Bloch electrons in a homogeneous electric field, *Phys. Rev. B* 38, 6322 (1988).
- [6] J. Feldmann, K. Leo, J. Shah, D.B.A. Miller, J.E. Cunningham, S. Schmitt-Rink, T. Meier, G. von Plessen, A. Schulze, and P. Thomas, Optical investigation of Bloch oscillations in a semiconductor superlattice, *Phys. Rev. B* 46, 7252 (1992).
- [7] C. Waschke, H.G. Roskos, R. Schwedler, K. Leo, H. Kurz, and K. Kohler, Coherent submillimeter-wave emission from Bloch oscillations in a semiconductor superlattice, *Phys. Rev. Lett.* 70, 3319 (1993).
- [8] G. Nenciu, Dynamics of band electrons in electric and magnetic fields: rigorous justification of the effective Hamiltonians, *Rev. Mod. Phys.* 63, 91 (1991).
- [9] C. Martijn de Sterke, J. N. Bright, Peter A. Krug, and T. E. Hammon, Observation of an optical Wannier-Stark ladder, *Phys. Rev. E* 57, 2365 (1998)
- [10] U. Peschel, T. Pertsch, and F. Lederer, Optical Bloch oscillations in waveguide arrays, *Opt. Lett.* 23, 1701 (1998).
- [11] A. Kavokin, G. Malpuech, A. Di Carlo, P. Lugli, and F. Rossi, Photonic Bloch oscillations in laterally confined Bragg mirrors, *Phys. Rev. B* 61, 4413 (2000)
- [12] G. Malpuech, A. Kavokin, G. Panzarini, and A. Di Carlo, Theory of photon Bloch oscillations in photonic crystals, *Phys. Rev. B* 63, 035108 (2001)
- [13] S Longhi, Optical Zener-Bloch oscillations in binary waveguide arrays, *Europhys. Lett.* 76 416 (2006)
- [14] T. Pertsch, P. Dannberg, W. Elflein, A. Brauer, and F. Lederer, Optical Bloch Oscillations in Temperature Tuned Waveguide Arrays, *Phys. Rev. Lett.* 83, 4752 (1999)
- [15] V. Agarwal, J. A. del Rio, G. Malpuech, M. Zamfirescu, A. Kavokin, D. Coquillat, D. Scalbert, M. Vladimirova, and B. Gil, Photon Bloch Oscillations in Porous Silicon Optical Superlattices, *Phys. Rev. Lett.* 92, 097401 (2004)
- [16] M. Ghulinyan, C.J. Oton, Z. Gaburro, L. Pavesi, C. Toninelli, and D.S. Wiersma, Zener Tunneling of Light Waves in an Optical Superlattice, *Phys. Rev. Lett.* 94, 127401 (2005)
- [17] S. Longhi, M. Lobino, M. Marangoni, R. Ramponi, P. Laporta, E. Cianci, and V. Foglietti, Semiclassical motion of a multiband Bloch particle in a time-dependent field: Optical visualization, *Phys. Rev. B* 74 155116 (2006)
- [18] C. Bersch, G. Onishchukov, and U. Peschel, Experimental observation of spectral Bloch oscillations, *Opt. Lett.* 34, 2372 (2009)
- [19] Xinyuan Qi, K.G. Makris, R. El-Ganainy, Peng Zhang, Jintao Bai, D.N. Christodoulides, and Zhigang Chen, Observation of accelerating Wannier–Stark beams in optically induced photonic lattices, *Opt. Lett.* 39, 1065 (2014)
- [20] Ye-Long Xu, W.S. Fegadolli, Lin Gan, Ming-Hui Lu, Xiao-Ping Liu, Zhi-Yuan Li, A. Scherer and Yan-Feng Chen, Experimental realization of Bloch oscillations in a parity-time synthetic silicon photonic lattice, *Nature Communications* volume 7, Article number: 11319 (2016)
- [21] I.L. Garanovich, S. Longhi, A.A. Sukhorukov, and Y.S. Kivshar, Light propagation and localization in modulated photonic lattices and waveguides *Physics Reports* 518 1 (2012)
- [22] M.B. Dahan, E. Peik, J. Reichel, Y. Castin, and C. Salomon, Bloch Oscillations of Atoms in an Optical Potential, *Phys. Rev. Lett.* 76, 4508 (1996).
- [23] S. Wilkinson, C. Bharucha, K. Madison, Q. Niu, and M. Raizen, Observation of Atomic Wannier-Stark Ladders in an Accelerating Optical Potential, *Phys. Rev. Lett.* 76, 4512 (1996).
- [24] H. R. Zhang and C. P. Sun, Bloch oscillations of polaritons of an atomic ensemble in magnetic fields, *Phys. Rev. A* 81, 063427 (2010)
- [25] Z.A. Geiger, K.M. Fujiwara, K. Singh, R. Senaratne, S.V. Rajagopal, M. Lipatov, T. Shimasaki, R. Driben, V.V. Konotop, T. Meier, and D.M. Weld, Observation and Uses of Position-Space Bloch Oscillations in an Ultracold Gas, *Phys. Rev. Lett.* 120, 213201 (2018).
- [26] Z. Pagel, W. Zhong, R.H. Parker, C.T. Olund, N.Y. Yao, and H. Muller, Symmetric Bloch oscillations of matter waves, *Phys. Rev. A* 102, 053312 (2020).
- [27] L. Masi, T. Petrucciani, G. Ferioli, G. Semeghini, G. Modugno, M. Inguscio, and M. Fattori, Spatial Bloch Oscillations of a Quantum Gas in a “Beat-Note” Superlattice, *Phys. Rev. Lett.* 127, 020601 (2021).
- [28] S. Longhi, Dynamic localization and Bloch oscillations in the spectrum of a frequency mode-locked laser, *Opt. Lett.* 30, 786 (2005)
- [29] S. Bahmani and A.N. Askarpour, Bloch oscillations and Wannier-Stark ladder in the coupled LC circuits, *Phys. Lett. A* 384, 126596 (2020).
- [30] G. Monsivais and R. Esquivel-Sirvent, Stark Ladder Resonances in Acoustic Waveguides, *Journal of Mechanics of Materials and Structures*, 2, 8, 1585 (2007).
- [31] G. Monsivais, R. Mendez-Sanchez, A. de Anda, J. Flores, L. Gutierrez, and A. Morales, Elastic Wannier–Stark Ladders in Torsional Waves *Journal of Mechanics of Materials and Structures*, 2, 1629 (2007)
- [32] N. Lanzillotti-Kimura, A. Fainstein, B. Perrin, B. Jusserand, O. Mauguin, L. Largeau, and A. Lemaitre, Bloch Oscillations of THz Acoustic Phonons in Coupled Nanocavity Structures, *Phys. Rev. Lett.* 104, 197402 (2010).

- [33] Y.-K. Liu, H.-W. Wu, P. Hu, and Z.-Q. Sheng, Spatial Bloch oscillations in acoustic waveguide arrays, *Appl. Phys. Express* 14, 064501 (2021).
- [34] A.R. Davoyan, I.V. Shadrivov, A.A. Sukhorukov, and Y.S. Kivshar, Plasmonic Bloch oscillations in chirped metal-dielectric structures, *Appl. Phys. Lett.* 94, 161105 (2009)
- [35] V. Kuzmiak, S. Eyderman, and M. Vanwolleghem, Controlling surface plasmon polaritons by a static and/or time-dependent external magnetic field, *Phys. Rev. B*, 86, 045403 (2012)
- [36] Bo Han Cheng, Yi-Chieh Lai, and Yung-Chiang Lan, Plasmonic Photonic Bloch Oscillations in Composite Metal-Insulator-Metal Waveguide Structure, *Plasmonics*, 9, 137 (2014)
- [37] V. Kuzmiak, A. A. Maradudin, and E. R. Mendez, Surface plasmon polariton Wannier-Stark ladder, *Opt. Lett.* 39, 1613 (2014)
- [38] A. Block, C. Etrich, T. Limboeck, F. Bleckmann, E. Soergel, C. Rockstuhl and S. Linden, Bloch oscillations in plasmonic waveguide arrays, *Nature Communications*, volume 5, Article number: 3843 (2014)
- [39] H. Wetter, Z. Fedorova, and S. Linden, Observation of the Wannier-Stark ladder in plasmonic waveguide arrays, *Optics Letters*, 47, 12, 3091 (2022)
- [40] H. Flayac, D. D. Solnyshkov, and G. Malpuech, Bloch oscillations of an exciton-polariton Bose-Einstein condensate, *Phys. Rev. B* 83, 045412 (2011)
- [41] H. Flayac, D. D. Solnyshkov, and G. Malpuech, Bloch oscillations of exciton-polaritons and photons for the generation of an alternating terahertz spin signal, *Phys. Rev. B*, 84, 125314 (2011)
- [42] J. Beierlein, O.A. Egorov, T.H. Harder, P. Gagel, M. Emmerling, C. Schneider, S. Hofling, U. Peschel, and S. Klemmt, Bloch Oscillations of Hybrid Light-Matter Particles in a Waveguide Array, *Adv. Opt. Mater.* 9, 2100126 (2021).
- [43] D. Cai, A.R. Bishop, and N. Gronbech-Jensen, Electric-Field-Induced Nonlinear Bloch Oscillations and Dynamical Localization, *Phys. Rev. Lett* 74, 1186 (1995).
- [44] R. Morandotti, U. Peschel, J.S. Aitchison, H.S. Eisenberg, and Y. Silberberg, Experimental observation of linear and nonlinear optical Bloch oscillations, *Phys. Rev. Lett.*, 83, 4756 (1999).
- [45] O. Morsch, J.H. Muller, M. Cristiani, D. Ciampini, and E. Arimondo, Bloch oscillations and mean-field effects of Bose-Einstein condensates in 1D optical lattices, *Phys. Rev. Lett.* 87, 140402 (2001).
- [46] M. Cristiani, O. Morsch, J.H. Muller, D. Ciampini, and E. Arimondo, Experimental properties of Bose-Einstein condensates in one-dimensional optical lattices: Bloch oscillations, Landau-Zener tunneling, and mean-field effects. *Phys. Rev. A* 65, 063612 (2002).
- [47] M. Gustavsson, E. Haller, M.J. Mark, J.G. Danzl, G. Rojas-Kopeinig, and H.-C. Nagerl, Control of Interaction-Induced Dephasing of Bloch Oscillations, *Phys. Rev. Lett.* 100, 080404 (2008).
- [48] Y.V. Bludov, V.V., Konotop, and M. Salerno, Dynamical localization of gap-solitons by time periodic forces. *EPL (Europhys. Lett.)* 87, 20004 (2009).
- [49] V.V. Konotop and M. Salerno, Modulation instability in Bose-Einstein condensates in optical lattices, *Phys. Rev.* 65, 021602 (2002).
- [50] M. Salerno, V.V. Konotop and Y.V. Bludov, Long-living Bloch oscillations of matter waves in periodic potentials, *Phys. Rev. Lett.* 101, 30405 (2008).
- [51] Y.V. Bludov, V.V. Konotop, and M. Salerno, Linear superpositions of nonlinear matter waves in optical lattices, *EPL (Europhys. Lett.)* 93, 30003 (2011).
- [52] C. Gaul, R.P.A. Lima, E. Diaz, C.A. Muller, and F. Domnguez-Adame, Stable Bloch oscillations of cold atoms with time-dependent interaction, *Phys Rev. Lett.* 102, 255303 (2009).
- [53] Y.V. Bludov, V.V. Konotop, and M. Salerno, Long-lived matter wave Bloch oscillations and dynamical localization by time-dependent nonlinearity management, *J. Phys. B* 42, 105302 (2009).
- [54] R. Driben, V.V. Konotop, T. Meier, and A.V. Yulin, Bloch oscillations sustained by nonlinearity, *Sci. Rep.* 7, 3194 (2017).
- [55] A. Yulin, R. Driben and T. Meier, Bloch oscillations and resonant radiation of light propagating in arrays of nonlinear fibers with high-order dispersion, *Phys. Rev. A* 96, 033827 (2017)
- [56] Kazuhisa Tomita, Chaotic response of nonlinear oscillators, *Physics Reports*, 86, 3, 113-167 (1982). *Physics Reports*
- [57] E. Shlizerman and V. Rom-Kedar, Three Types of Chaos in the Forced Nonlinear Schrodinger Equation, *Phys. Rev. Lett.* 96, 024104 (2006).
- [58] E. Shlizerman and V. Rom-Kedar, Classification of solutions of the forced periodic nonlinear Schrodinger equation, *Nonlinearity*, 23, 2183 (2010).
- [59] V. Achilleos, A.R. Bishop, S. Diamantidis, D.J. Frantzeskakis, T.P. Horikis, N.I. Karachalios, and P.G. Kevrekidis, Dynamical playground of a higher-order cubic Ginzburg-Landau equation: From orbital connections and limit cycles to invariant tori and the onset of chaos, *Phys. Rev. E*, 94, 012210 (2016).
- [60] P.P. Galuzio, S. Benkadda, and S.R. Lopes, Characterization of intermittency at the onset of turbulence in the forced and damped nonlinear Schrödinger equation, *Communications in Nonlinear Science and Numerical Simulation*, 42, 404 (2017).